JACS
JOURNAL OF THE AMERICAN CHEMICAL SOCIETY
pubs.acs.org/JACS
Article

Photothermal Mediated Chemical Recycling to Monomers via Carbon Quantum Dots

Liat H. Kugelmass, Clotilde Tagnon, and Erin E. Stache*

Cite This: J. Am. Chem. Soc. 2023, 145, 16090−16097
Read Online
ACCESS | Metrics & More | Article Recommendations | Supporting Information

ABSTRACT: Plastic recycling strategies to combat rapidly increasing waste buildup are of utmost environmental importance. Chemical recycling to monomers has emerged as a powerful strategy that enables infinite recyclability through depolymerization. However, methods for chemical recycling to monomers typically rely on bulk heating of polymers, which leads to unselective depolymerization in complex polymer mixtures and the formation of degradation byproducts. Here, we report a selective chemical recycling strategy facilitated by photothermal carbon quantum dots under visible light irradiation. Upon photoexcitation, we found that carbon quantum dots generate thermal gradients that induce depolymerization of various polymer classes, including commodity and postconsumer waste plastics, in a solvent-free system. This method also provides selective depolymerization in a mixture of polymers, not possible by bulk heating alone, enabled by localized photothermal heat gradients and the subsequent spatial control imparted over radical generation. Photothermal conversion by metal-free nanomaterials facilitates chemical recycling to monomers, an important approach in addressing the plastic waste crisis. More broadly, photothermal catalysis enables challenging C−C bond cleavages with the generality of heating but without indiscriminate side reactions typical of bulk thermolysis processes.

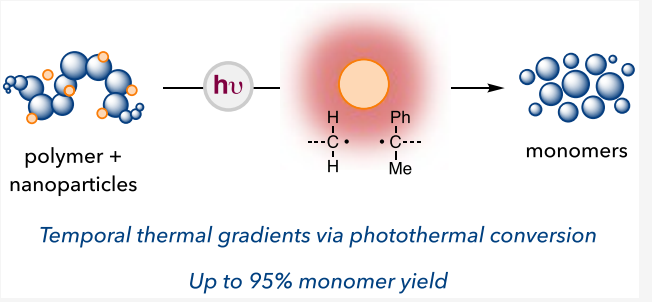

INTRODUCTION

While plastics have enabled modern society, the lack of recycling has led to waste buildup, which is expected to double by 2050.[1] Mechanical recycling can be effective for some commodity polymers, but there are significant limitations to its widespread implementation, including the deterioration of polymer properties after repeated processing.[2] In comparison, chemical recycling to monomers (CRM) enables infinite recyclability by regenerating virgin materials.[3] While methods such as dilution in solvent to depress the ceiling temperature (T_c)[4] or catalyst addition can enhance depolymerization kinetics under mild conditions,[5] heating remains the most general strategy for depolymerization. However, bulk heating polymers under ambient conditions may lead to oxidized byproducts due to the unselective formation of reactive intermediates (Figure 1a).[6−10] Additionally, bulk heating precludes selectivity among polymers in a mixture, which is a typical complexity in real-world waste streams.[2]

Visible light photochemistry has enabled selective reactions via energy or electron transfer.[11−13] The selectivity arises from the inherent redox properties of the reactants with required proximity to a photocatalyst, providing spatial and temporal control over reactive intermediates. An underused strategy in synthetic photochemistry is the photothermal effect. This phenomenon arises from the irradiation of chromophores with visible or near-infrared light to access an excited state species that relaxes to the ground state through a nonradiative decay pathway.[14,15] This light-to-heat conversion process allows photons in the visible region to realize extreme temperatures localized to the chromophore while maintaining lower bulk temperatures. We hypothesized that in contrast to conventional bulk heating, where all molecules and reaction media are uniformly thermally excited, resulting in high concentrations of reactive intermediates, photothermal heating would preferentially heat the molecules directly adjacent to the chromophore, confining the formation of reactive intermediates (Figure 1b).

We wanted to leverage this phenomenon to perform challenging chemical transformations. For example, a C−C bond with an activation barrier of 35 kcal/mol would be cleaved at temperatures >270 °C on a meaningful timescale but would remain bonded at lower temperatures. By implementing photothermal heating, C−C bond cleavage would only proceed proximally to the chromophore. Spatially confined C−C bond cleavage should result in a lower concentration of reactive radical intermediates, limiting side reactions, such as bimolecular oxidation reactions. This

Received: April 28, 2023
Published: July 11, 2023

https://doi.org/10.1021/jacs.3c04448
J. Am. Chem. Soc. 2023, 145, 16090−16097

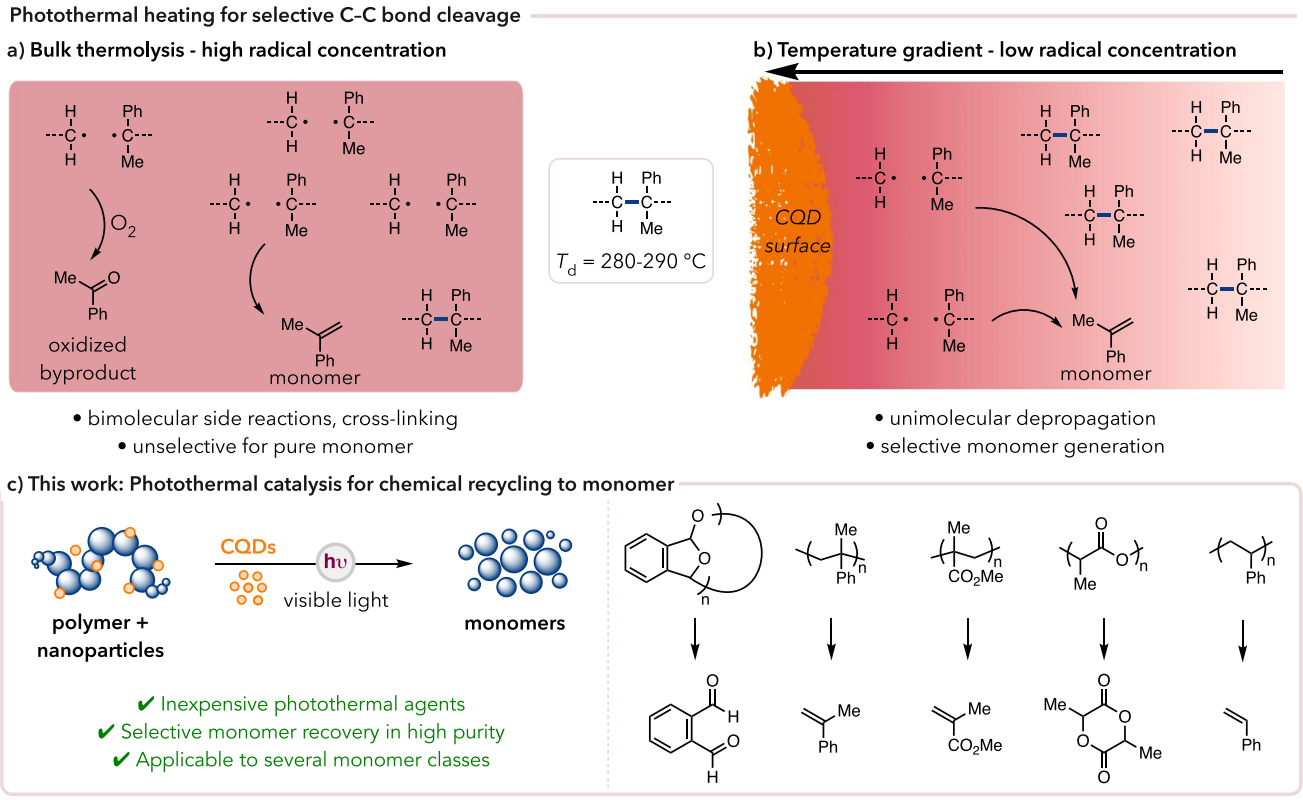

Figure 1. (a) Bulk heating generates high radical concentrations and facilitates bimolecular byproduct reactions. (b) Temperature gradients generated through photothermal conversion provide low radical concentrations. (c) Use of CQDs for photothermal conversion and scope of polymers amenable to photothermal depolymerization.

concept is supported by recent work, which has shown electrically generated thermal gradients to promote the pyrolysis of select polymers to monomers with improved yield and selectivity compared to uniform heating.[16] We hypothesized that photothermal heating could merge the advantages of photocatalysis—the temporal and spatial control over radical formation—with the generality of heat to perform challenging transformations like C−C bond cleavages in depolymerization reactions.[17] We envisioned that this method could be applied broadly over several classes of polymers, both through direct thermal C−C bond cleavage and in combination with additional catalysts to affect CRM (Figure 1c).

To test this concept, we needed to identify a photothermal agent that could facilitate the depolymerization of common plastics to monomers. Previous reports have examined metallic photothermal nanoparticles (NPs), synthesized from gold, silver, and iron, for unselective polymer degradation without depolymerization.[18a−f] Recently, carbon-based NPs were reported to promote photothermal depolymerization, using designer carbon nanotubes for polymer glycolysis of polyethylene terephthalate.[18g] Though these works present notable advances in photothermal catalysis, a general strategy for depolymerization to monomers has not been reported. We envisioned using inexpensive and readily available carbon-based NPs, such as carbon quantum dots (CQDs), as photothermal agents for depolymerization. CQDs exhibit highly tunable absorption and photoluminescence properties based on carbon source, size, and surface modification.[19,20] While CQDs are typically used for energy or electron transfer applications in sensors,[21] drug delivery,[22] and photoredox catalysis,[23] emerging work has shown promising photothermal conversion abilities.[24] We hypothesized that CQDs would be able to produce high-temperature photothermal gradients capable of inducing depolymerization.

We searched for materials with low fluorescence quantum yield to identify potential photothermal CQDs, hypothesizing that they were engaging in nonradiative decay.[25] Wang and coworkers described a formulation using metal-free hydrothermal treatment of L-ascorbic acid (vitamin C) to prepare CQDs with modest photoluminescent properties.[26] To test the photothermal ability of these CQDs for chemical recycling to monomers, we began our initial depolymerization studies with poly(α-methyl styrene) (PAMS), which displays a moderately high degradation temperature (T_d = 280 °C) yet facile depolymerization to monomer due to its modest ceiling temperature (T_c = 61 °C) and propagating tertiary radical intermediate.[6,27,28]

RESULTS AND DISCUSSION

Identification of Conditions. In initial studies, we interspersed CQDs (10 wt % with respect to the polymer) in PAMS (M_n = 135 kDa) by solvent-casting films from tetrahydrofuran (THF). After irradiating a 10 mg film sample over broad-spectrum white (color temperature of 6000 K) light-emitting diodes (LEDs) for 30 min under an ambient atmosphere, we recovered 66% monomer with only minimal oxidative byproduct (<1% acetophenone) and with the remaining polymer displaying a significant reduction in molecular weight by gel permeation chromatography (GPC) (Figure 2a, entry 1). Irradiation of the polymer film without CQDs did not induce depolymerization or degradation (Table

https://doi.org/10.1021/jacs.3c04448
J. Am. Chem. Soc. 2023, 145, 16090−16097

a)

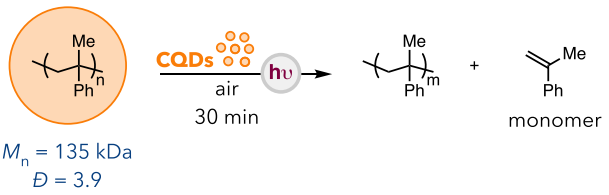

M_n = 135 kDa
$Đ$ = 3.9

entry[a]	conditions	M_n (kDa)	$Đ$	% monomer
1	solvent cast	12	4.5	66
2	powder mixture	18	5.9	65
3[b]	solvent free	13	3.8	44
4[c]	gram scale	29	6.6	73
5[d]	vacuum distillation	67	6.5	85

b)

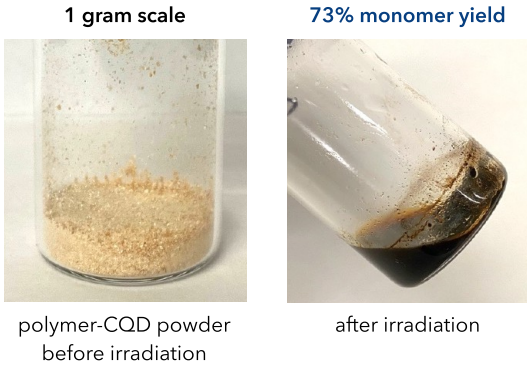

Figure 2. (a) Variations in the procedure to eliminate solvent use, scale-up, and isolation of the monomer. [a]10 mg of the polymer, 10 wt % CQDs; [b]30 wt % dry CQDs, PAMS M_n = 23.5 kDa; [c]60 min; [d]50 mg of the polymer. (b) Scale-up to one gram of the polymer on a PAMS-CQD powder mixture. See the Supporting Information for full experimental details.

S1, entry 3). Further, the polymer-CQD film was stable in the dark while exposed to background heat from the light source, signifying that both light and CQDs are necessary to trigger depolymerization (Table S1, entry 4).

Considering practical implementation, we sought to expand our method beyond single-layer films. Irradiation of PAMS powder directly mixed with a highly concentrated solution of CQDs (10 wt %) in THF afforded a high monomer yield (65%), comparable to film experiments (Figure 2a, entry 2). Further, irradiation of PAMS powder manually mixed with dry CQDs (30 wt %) afforded monomer, albeit with decreased yields, showing promise for fully solvent-free processing upon further optimization (Figure 2a, entry 3). Using the polymer powder mixing protocol, we demonstrated the scalability of our photothermal depolymerization method, achieving a high monomer yield (73%) on a gram scale (Figure 2a, entry 4, and Figure 2b). Additionally, our protocol was conducive to a distillation setup, where light was employed instead of a traditional heating source. We successfully invoked vacuum distillation of the monomer from PAMS-CQD (10 wt %) powder by photothermal heating, where the monomer was isolated in 85% yield with high purity (Figure 2a, entry 5). We attribute the increased yields to greater heat retention by larger masses of the polymer and CQDs. Excitingly, this built-in purification step improves the practicality of our method for closed-loop CRM and allows for the removal and isolation of more reactive monomers.

With the successful implementation of our protocol, we compared our photothermal heating strategy to conventional bulk heating using PAMS (Figure 3). Upon bulk heating of the

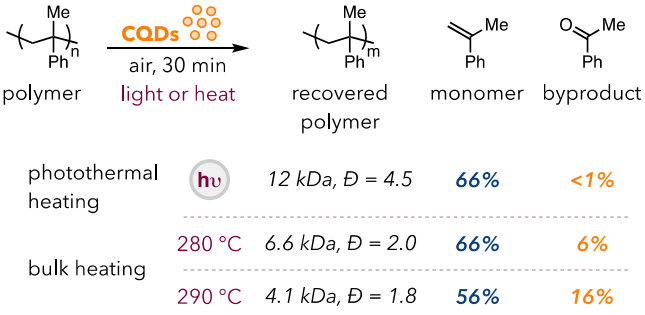

Figure 3. Comparison of PAMS depolymerization product distribution under photothermal and bulk heating conditions. See the Supporting Information for full experimental details.

PAMS-CQD (10 wt %) film under air for 30 min, trace monomer was observed at 250 °C and was only formed in considerable amounts above 270 °C (Figure S68 and Table S9), in agreement with experimentally determined T_d (280 °C) by thermogravimetric analysis (TGA) (Figure S39). After uniform heating at 280 °C, the monomer was observed in 66% yield, comparable to our photothermal method. However, an increase in the oxidized byproduct acetophenone was also observed (6% yield). More strikingly, when heated to 290 °C, the monomer yield decreased to 56%, and the byproduct yield increased to 16%. Despite the identical atmospheric conditions, our photothermal method yielded <1% oxidized byproduct, highlighting a significant distinction between bulk and photothermal heating (Tables S1 and S9). We hypothesize that cleaner depolymerization to monomers is achieved under photothermal conditions due to localized heat gradients that allow reactions to proceed at lower effective bulk temperatures. The resulting lower reactive intermediate concentrations should reduce byproduct pathways like bimolecular reactions with oxygen (Figure 1a). Additionally, heat localization to the polymer material may allow for better monomer diffusion away from elevated temperatures compared to bulk heating, limiting byproduct formation.[16]

Mechanistic Discussion. We note that a photoinduced thermal depolymerization mechanism is most probable. Additional mechanistic studies are inconsistent with single electron transfer, energy transfer,[29] or hydrogen atom abstraction[30] mechanisms. We observed no fluorescence quenching of CQDs with isopropylbenzene, a model polymer repeat unit of PAMS (Figures S24–S35), which would occur if the polymer was quenching the excited state of the CQDs to activate the polymer backbone for depolymerization. A charge-transfer complex was also not observed in UV/vis studies (Figures S16 and S17). Further, treatment of PAMS with eosin Y, a photocatalyst known for generating singlet oxygen, only afforded acetophenone and polymer chain cleavage, with no monomer observed under ambient conditions (Figure S36). This study negates a mechanism where the excited state of the CQDs is quenched with oxygen to afford singlet oxygen or superoxide, which could abstract an H-atom from the polymer backbone, followed by depolymerization. Lastly, TGA showed comparable T_d for PAMS with and without CQDs, in agreement with the temperature at which monomer generation

https://doi.org/10.1021/jacs.3c04448
J. Am. Chem. Soc. 2023, 145, 16090−16097

was observed upon bulk heating (Figures S39 and S68 and Table S9).

Kinetics and CQD Analysis. Observing a visual change to the CQDs after irradiation (Figure 2b) and limited thermal stability by TGA (Figure S23), we sought to better understand the role of CQDs as a photothermal agent and any changes occurring throughout depolymerization. We performed kinetic trials of PAMS photothermal depolymerization with CQDs (10 wt %). We observed a rapid increase in the monomer yield over the first 5 min of irradiation. Yields varied at increased reaction times but generally were observed to peak at 30 min (Figure 4a). We note that our maximum monomer yield

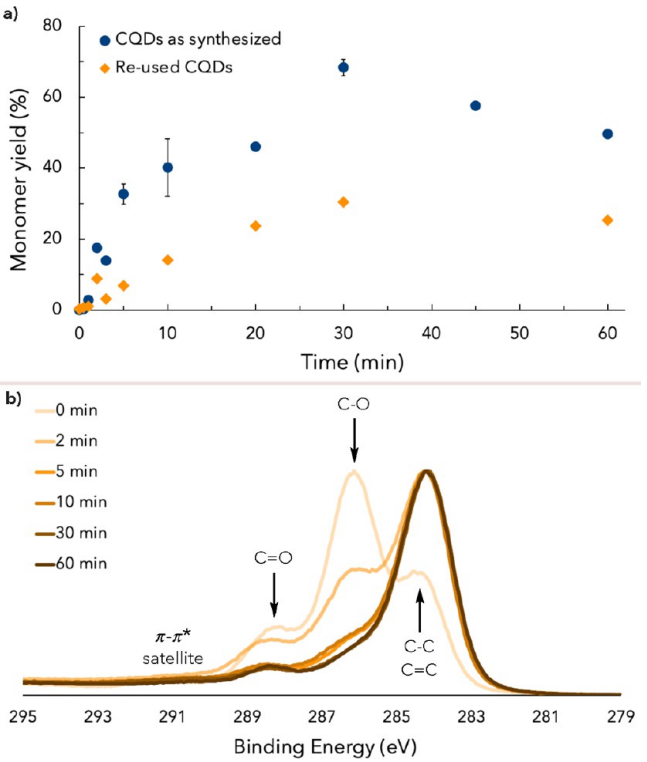

Figure 4. Depolymerization kinetics and CQD structural changes. (a) Depolymerization kinetics of PAMS with CQDs and reused CQDs. Error bars denote standard deviation for triplicate trials. (b) Loss of the C−O surface functionality in CQDs with irradiation time, observed by XPS.

(75%) in these kinetic trials was slightly higher than in previous experiments of a similar scale, which we attribute to the lower molecularweight polymer sample used (M_n = 23.5 kDa), which should have faster kinetics under a chain unzipping mechanism.

We hypothesized that the CQDs are further carbonized upon photothermal heat generation, losing the oxygenated surface functionality and resulting in higher relative carbon composition. Indeed, by X-ray photoelectron spectroscopy (XPS) and infrared spectroscopy (IR), we observed a rapid loss of both the oxygen content and C−O bond features within the first 10 min of reaction time, supporting our carbonization hypothesis (Figure 4b and Figures S58−S66). Loss of the oxygen surface functionality may benefit more reactive depolymerization intermediates since the CQD surface would be less reactive. Because monomer generation is observed after 10 min of reaction time, we presume that the carbonized CQDs are still active photothermal agents. To test this hypothesis, we reused CQDs isolated from a previous PAMS-CQD photothermal depolymerization reaction. However, we found that the reused CQDs enabled PAMS depolymerization upon irradiation, with reduced monomer yields (30% at 30 min) (Figure 4a), although the kinetic profile was similar. Additionally, depolymerization continued in light on−off studies, further supporting that the carbonized CQDs are still photothermally active (Table S8 and Figure S67). Since monomer yields were not appreciably lower in the light on−off studies compared to constant irradiation experiments, we speculate that the decreased yields with reused CQDs are related to the observed poorer dispersion in the polymer.

Polymer Scope. We tested the generality of this approach with different polymer substrates. We began by examining the depolymerization of polyphthalaldehyde (PPA), a polymer used for photoresists that has a low T_d (160 °C) (Figure S12) and T_c (−36 °C).[31] Upon white light irradiation of the PPA (20 mg, M_n = 31 kDa) film interspersed with CQDs (10 wt %), we isolated 58% *ortho*-phthaldialdehyde monomer (Table S10, entry 3). However, we observed monomer photodegradation due to shorter wavelengths (blue light region) in the broad-spectrum white light source (Table S10 and Figure S111), a known degradation pathway of *o*-phthaldialdehyde.[32] Consequently, 525 nm irradiation afforded the monomer in 78% yield without photodegradation (Figure 5 and Table S10).

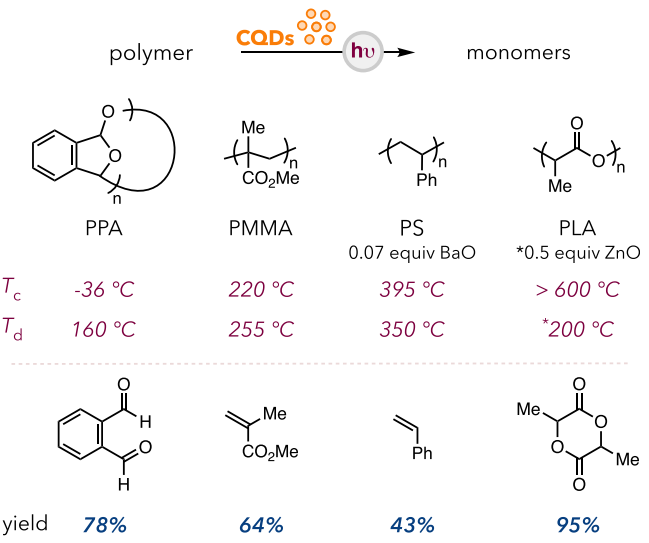

Figure 5. Expansion to several classes of polymers. Photothermal depolymerization of polyphthalaldehyde (PPA), poly(methyl methacrylate) (PMMA), polystyrene (PS), and poly(lactic acid) (PLA) to corresponding monomers. See the Supporting Information for full experimental details.

Next, we looked at the depolymerization of commercial poly(methyl methacrylate) (PMMA), which has a similar T_d (255 °C)[28] but a considerably higher T_c (220 °C)[27] than PAMS. Depolymerization of poly(methyl methacrylate) occurs efficiently at temperatures >400 °C under an inert atmosphere.[8,33] Like PAMS, PMMA depolymerization proceeds through a propagating tertiary radical intermediate. However, the proximity of the T_c to the T_d and unproductive reactions such as oxidation, cross-linking, and auto-polymerization at elevated temperatures create a more challenging system.[8] We subjected a solvent-cast mixture of commercial PMMA (50 mg, M_n = 25 kDa) and CQDs (10 wt %) to white light

https://doi.org/10.1021/jacs.3c04448
J. Am. Chem. Soc. 2023, 145, 16090−16097

irradiation in the vacuum distillation setup to isolate the methyl methacrylate monomer directly into butylated hydroxytoluene (BHT) polymerization inhibitor. Excitingly, after 4 h of irradiation with white light, we isolated 64% monomer (Figure 5 and Table S11).

More demonstrative of real-world recycling demands, we applied our method to various commercial polymers and postconsumer waste plastics. Depolymerization of poly(lactic acid) (PLA) was particularly interesting because it is currently the most widely used biorenewable plastic, produced at over 140,000 tons annually.[3,34] Due to its extremely high T_c (>600 °C), PLA undergoes side reactions such as elimination and epimerization preferentially over depolymerization when heated.[9,35] However, by employing a catalyst, PLA depolymerization to L-lactide monomer can be achieved in bulk at lower temperatures (~200 °C).[35] With the incorporation of ZnO (0.5 equiv with respect to the monomer repeat unit) and 5 wt % CQDs, we were able to generate 95% lactide (90% as L-lactide versus *meso*-lactide) from a postconsumer PLA 3D printer filament (50 mg, M_n = 115 kDa, filtered to remove composites/dyes) under white LED irradiation for 4 h (Figure 5 and Table S12), demonstrating the compatibility of photothermal catalysis with other catalytic agents.

Lastly, we turned to polystyrene (PS), a commodity polymer annually produced on a megaton scale. With a recycling rate of <1%, PS accounts for a third of the world's landfills by volume.[36] PS presents a significant challenge to CRM due to its high T_d (350 °C) with even higher T_c (395 °C), for which meaningful depolymerization must occur at temperatures >400 °C.[37] Furthermore, due to highly reactive radical intermediates, PS undergoes significant random chain scission events (versus chain unzipping), cross-linking, auto-polymerization of monomers, and complex byproduct formation (α-methyl styrene, toluene, acetophenone, benzoic acid, benzaldehyde, styrene dimers, styrene trimers, etc.).[10,28] However, with the addition of a catalyst, styrene monomer is known to be generated in moderate to high yields under pyrolysis at 350−450 °C.[38] Remarkably, with our simple photothermal vacuum distillation protocol (20 wt % CQDs, 0.07 equiv of BaO), postconsumer PS (25 mg, Hefty clear lid, M_n = 105 kDa) was converted to styrene monomer in 43% yield after 2 h of irradiation with white LEDs (Figure 5 and Table S15).

Postconsumer Polymer Recycling. Various postconsumer waste PS products were subjected to our method (20 wt % CQDs, 1 equiv of ZnO), including foamed PS and composite-containing samples, yielding 22−50% styrene (Figure 6a). In contrast to specialized pyrolysis equipment operated at temperatures of >400 °C, only a simple LED source and standard short-path distillation glassware were used here. Further, we incorporated postconsumer PLA with CQDs and ZnO by a thermoforming technique, eliminating solvent usage. CQDs (5 wt %) and ZnO (0.5 equiv) were interspersed in PLA using a Carver press, with a negligible impact on M_n (Figures S45-S47). This thermoformed material was subjected to white light irradiation under vacuum distillation to recover 81% lactide (Table S14, entry 5). An identical trial with a used beverage cup made from PLA provided 91% lactide (Figure 6b and Table S14, entry 1). Gratifyingly, thermoformed PLA samples provided comparable monomer yields to solvent-cast samples (~80% lactide) at even lower CQDs and ZnO loadings, 2.5 wt % and 0.25 equiv, respectively (Table S14).

Spatial Control. We hypothesized that the spatial control imparted by photothermal conversion could enable selective

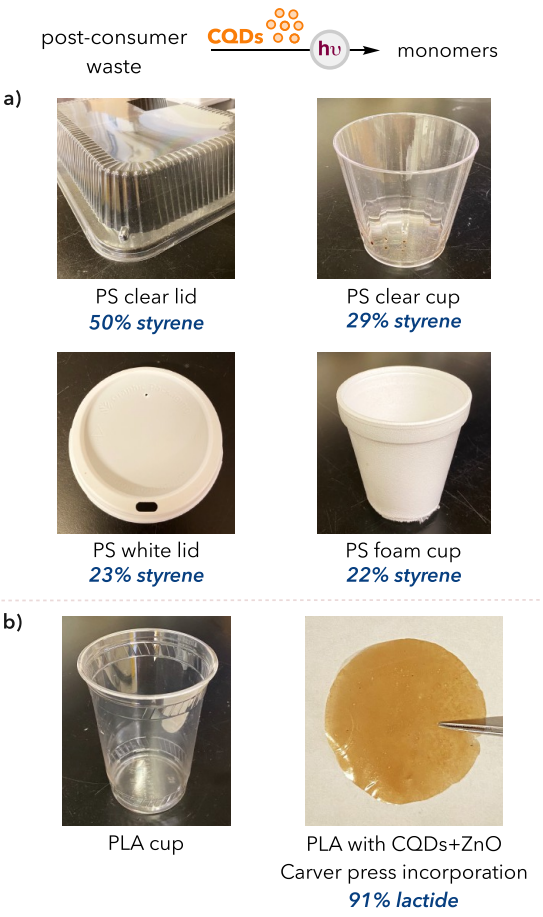

Figure 6. (a) Images of postconsumer waste PS and monomer yields under 20 wt % CQDs and 1 equiv of ZnO conditions. (b) Images of postconsumer waste PLA, thermoformed with CQDs and ZnO, and monomer yield. See the Supporting Information for full experimental details.

depolymerization of one polymer in a mixed polymer system, a common complexity in real-world plastic waste streams.[2] To explore this, we prepared a mixture of PAMS interspersed with CQDs and commercial PMMA or PS absent of CQDs. When subjected to visible light irradiation, we observed the formation of the α-methyl styrene monomer in good yields (51 and 74% in the presence of PMMA and PS, respectively) with no depolymerization or degradation of the commercial polymers. In contrast, when bulk heated to 290 °C, both polymers in the mixture degraded without selectivity toward CQD incorporation. Alongside PAMS depolymerization, PMMA was depolymerized to monomer in 54% yield, and PS was cleaved into shorter chains and small molecules (Figure 7a−c, Tables S18−S20, and Figures S88−S93). These results demonstrate the utility of photothermal heating with localized heat gradients to enable selective depolymerization in mixed polymer waste streams.

CONCLUSIONS

Herein, we have demonstrated the use of photothermal catalysis for application in CRM with high monomer selectivity, in contrast to bulk heating. This method was successfully implemented with five distinct polymer classes, including commercial samples and postconsumer waste plastics of commodity polymers. Furthermore, the spatial and temporal control afforded by photothermal catalysis allowed for selective

https://doi.org/10.1021/jacs.3c04448
J. Am. Chem. Soc. 2023, 145, 16090−16097

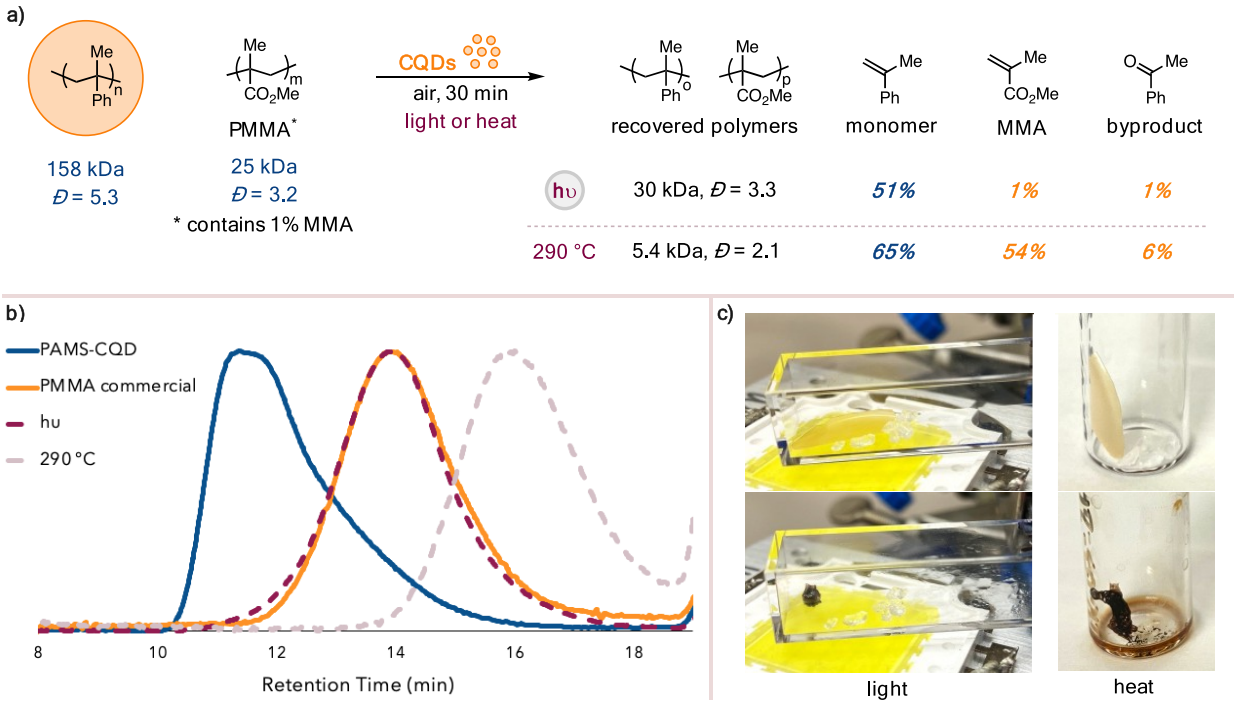

Figure 7. Selective depolymerization in a mixed polymer system. (a) Comparison of PAMS-CQD and PMMA depolymerization product distribution under photothermal and bulk heating conditions. (b) GPC traces of starting polymers and remaining polymers after irradiation and heating. (c) Images of the mixed polymer system before and after irradiation and heating. See the Supporting Information for full experimental details.

depolymerization in complex plastic waste streams. Additionally, we studied the compositional changes to CQDs during photothermal heating to better understand this material as a photothermal agent. Together, this work shows how photothermal conversion of CQDs can be utilized for challenging chemical transformations such as C−C bond cleavages with more control than conventional bulk heating methods due to localized heat gradients and reduced concentration of reactive radical intermediates.

■ ASSOCIATED CONTENT

Supporting Information

The Supporting Information is available free of charge at https://pubs.acs.org/doi/10.1021/jacs.3c04448.

Experimental details, methods, data, and photographs of the experimental setup (PDF)

■ AUTHOR INFORMATION

Corresponding Author

Erin E. Stache − *Department of Chemistry and Chemical Biology, Cornell University, Ithaca, New York 14853, United States;* orcid.org/0000-0002-4670-9117; Email: ees234@cornell.edu

Authors

Liat H. Kugelmass − *Department of Chemistry and Chemical Biology, Cornell University, Ithaca, New York 14853, United States*

Clotilde Tagnon − *Department of Chemistry and Chemical Biology, Cornell University, Ithaca, New York 14853, United States;* orcid.org/0000-0002-6544-5620

Complete contact information is available at: https://pubs.acs.org/10.1021/jacs.3c04448

Notes

The authors declare the following competing financial interest(s): E.E.S and L.H.K are inventors on US provisional letters patent application 10415: 63/383,419, submitted by Cornell University, the status of which is pending, which covers the methods in this paper. The remaining authors declare no competing financial interest.

■ ACKNOWLEDGMENTS

We thank the Coates, Hyster, Milner, and Chen groups at Cornell for use of their equipment. This work was funded by Cornell University and the President's Council of Cornell Women Affinito−Stewart Grant (L.H.K.). In addition, this work made use of the NMR Facility at Cornell University, supported, in part, by the National Science Foundation through MRI Award CHE-1531632 and the Cornell Center for Materials Research Facilities, supported by National Science Foundation Award DMR-1719875.

■ REFERENCES

(1) Geyer, R.; Jambeck, J. R.; Law, K. L. Production, use, and fate of all plastics ever made. *Sci. Adv.* **2017**, *3*, No. e1700782.

(2) Ragaert, K.; Delva, L.; Van Geem, K. Mechanical and chemical recycling of solid plastic waste. *Waste Manage.* **2017**, *69*, 24−58.

(3) Coates, G. W.; Getzler, Y. D. Y. L. Chemical recycling to monomer for an ideal, circular polymer economy. *Nat. Rev. Mater.* **2020**, *5*, 501−516.

(4) (a) Wang, H. S.; Truong, N. P.; Pei, Z.; Coote, M. L.; Anastasaki, A. Reversing RAFT polymerization: Near-quantitative monomer generation via a catalyst-free depolymerization approach. *J. Am. Chem. Soc.* **2022**, *144*, 4678−4684. (b) Young, J. B.; Bowman, J. I.; Eades, C. B.; Wong, A. J.; Sumerlin, B. S. Photoassisted radical depolymerization. *ACS Macro Lett.* **2022**, *11*, 1390−1395.

(5) (a) Abel, B. A.; Snyder, R. L.; Coates, G. W. Chemically recyclable thermoplastics from reversible-deactivation polymerization

of cyclic acetals. *Science* **2021**, *373*, 783−789. (b) Hester, H. G.; Abel, B. A.; Coates, G. W. Ultra-High-Molecular-Weight Poly(Dioxolane): Enhancing the Mechanical Performance of a Chemically Recyclable Polymer. *J. Am. Chem. Soc.* **2023**, *145*, 8800−8804. (c) Bellotti, V.; Parkatzidis, K.; Wang, H. S.; Watuthanthrige, N. D. A.; Orfano, M.; Monguzzi, A.; Truong, N. P.; Simonutti, R.; Anastasaki, A. Light-accelerated depolymerization catalyzed by Eosin Y. *Polym. Chem.* **2023**, *14*, 253−258.

(6) Madras, G.; Smith, J. M.; McCoy, B. J. Thermal degradation of poly(α-methylstyrene) in solution. *Polym. Degrad. Stab.* **1996**, *52*, 349−358.

(7) Jellinek, H. H. G.; Kachi, H. Thermal degradation of poly(α-methyl styrene) in a closed system. *J. Polym. Sci., Part C: Polym. Symp.* **1968**, *23*, 97−108.

(8) Godiya, C. B.; Gabrielli, S.; Materazzi, S.; Pianesi, M. S.; Stefanini, N.; Marcantoni, E. Depolymerization of waste poly(methyl methacrylate) scraps and purification of depolymerized products. *J. Environ. Manage.* **2019**, *231*, 1012−1020.

(9) Tang, X.; Chen, E. Y.-X. Toward infinitely recyclable plastics derived from renewable cyclic esters. *Chem* **2019**, *5*, 284−312.

(10) Achilias, D. S.; Kanellopoulou, I.; Megalokonomos, P.; Antonakou, E.; Lappas, A. A. Chemical recycling of polystyrene by pyrolysis: Potential use of the liquid product for the reproduction of polymer. *Macromol. Mater. Eng.* **2007**, *292*, 923−934.

(11) Corrigan, N.; Shanmugam, S.; Xu, J.; Boyer, C. Photocatalysis in organic and polymer synthesis. *Chem. Soc. Rev.* **2016**, *45*, 6165−6212.

(12) Shaw, M. H.; Twilton, J.; MacMillan, D. W. C. Photoredox catalysis in organic chemistry. *J. Org. Chem.* **2016**, *81*, 6898−6926.

(13) Staveness, D.; Bosque, I.; Stephenson, C. R. J. Free radical chemistry enabled by visible light-induced electron transfer. *Acc. Chem. Res.* **2016**, *49*, 2295−2306.

(14) Cui, X.; Ruan, Q.; Zhuo, X.; Xia, X.; Hu, J.; Fu, R.; Li, Y.; Wang, J.; Xu, H. Photothermal nanomaterials: A powerful light-to-heat converter. *Chem. Rev.* **2023**, *123*, 6891−6952.

(15) (a) Wu, X.; Chen, G. Y.; Owens, G.; Chu, D.; Xu, H. Photothermal materials: A key platform enabling highly efficient water evaporation driven by solar energy. *Mater. Today Energy* **2019**, *12*, 277−296. (b) Chu, C.; Ryberg, E. C.; Loeb, S. K.; Suh, M.-J.; Kim, J.-H. Water disinfection in rural areas demands unconventional solar technologies. *Acc. Chem. Res.* **2019**, *52*, 1187−1195.

(16) During submission of this manuscript an electrical variant of temporal gradient heating was disclosed: Dong, Q.; Lele, A. D.; Zhao, X.; Li, S.; Cheng, S.; Wang, Y.; Cui, M.; Guo, M.; Brozena, A. H.; Lin, Y.; Li, T.; Xu, L.; Qi, A.; Kevrekidis, I. G.; Mei, J.; Pan, X.; Liu, D.; Ju, Y.; Hu, L. Depolymerization of plastics by means of electrified spatiotemporal heating. *Nature* **2023**, *616*, 488−494.

(17) (a) Van Burns, E. N.; Lear, B. J. Controlled rapid formation of polyurethane at 700 K: Thermodynamic and kinetic consequences of extreme photothermal heating. *J. Phys. Chem. C* **2019**, *123*, 14774−14780. (b) Phillips, S. J.; Ginder, N. C.; Lear, B. J. Rapid photothermal synthesis of polyurethane from blocked isocyanates. *Macromolecules* **2022**, *55*, 7232−7239. (c) Haas, K. M.; Lear, B. J. Billion-fold rate enhancement of urethane polymerization via the photothermal effect of plasmonic gold nanoparticles. *Chem. Sci.* **2015**, *6*, 6462−6467. (d) Fasciani, C.; Alejo, C. J. B.; Grenier, M.; Netto-Ferreira, J. C.; Scaiano, J. C. High-temperature organic reactions at room temperature using plasmon excitation: Decomposition of dicumyl peroxide. *Org. Lett.* **2011**, *13*, 204−207. (e) Steinhardt, R. C.; Steeves, T. M.; Wallace, B. M.; Moser, B.; Fishman, D. A.; Esser-Kahn, A. P. Photothermal nanoparticle initiation enables radical polymerization and yields unique, uniform microfibers with broad spectrum light. *ACS Appl. Mater. Interfaces* **2017**, *9*, 39034−39039. (f) Bakhtiari, A. B. S.; Hsiao, D.; Jin, G.; Gates, B. D.; Branda, N. R. An efficient method based on the photothermal effect for the release of molecules from metal nanoparticle surfaces. *Angew. Chem., Int. Ed.* **2009**, *48*, 4166−4169.

(18) (a) Johnson, R. J. G.; Haas, K. M.; Lear, B. J. Fe_3O_4 nanoparticles as robust photothermal agents for driving high barrier reactions under ambient conditions. *Chem. Commun.* **2015**, *51*, 417−420. (b) Haas, K. M.; Lear, B. J. Degradation of polypropylene carbonate through plasmonic heating. *Nanoscale* **2013**, *5*, 5247−5251. (c) Firestone, G.; Huang, H.; Bochinski, J. R.; Clarke, L. I. Photothermally-driven thermo-oxidative degradation of low density polyethylene: heterogeneous heating plus a complex reaction leads to homogeneous chemistry. *Nanotechnology* **2019**, *30*, 475706. (d) Kim, Y. J.; Park, B. C.; Park, J.; Kim, H.-D.; Kim, N. H.; Suh, Y. D.; Kim, Y. K. White-light-emitting magnetite nanoparticle−polymer composites: Photonic reactions of magnetic multi-granule nanoclusters as photothermal agents. *Nanoscale* **2016**, *8*, 17136−17140. (e) Huang, H.; Firestone, G.; Fontecha, D.; Gorga, R. E.; Bochinski, J. R.; Clarke, L. I. Nanoparticle-based photothermal heating to drive chemical reactions within a solid: Using inhomogeneous polymer degradation to manipulate mechanical properties and segregate carbonaceous byproducts. *Nanoscale* **2020**, *12*, 904−923. (f) Johnson, R. J. G.; Schultz, J. D.; Lear, B. J. Photothermal effectiveness of magnetite nanoparticles: Dependence upon particle size probed by experiment and simulation. *Molecules* **2018**, *23*, 1234. (g) Liu, Y.; Zhong, Q.; Xu, P.; Huang, H.; Yang, F.; Cao, M.; He, L.; Zhang, Q.; Chen, J. Solar thermal catalysis for sustainable and efficient polyester upcycling. *Matter* **2022**, *5*, 1305−1317.

(19) (a) Wang, X.; Feng, Y.; Dong, P.; Huang, J. A mini review on carbon quantum dots: Preparation, properties, and electrocatalytic application. *Front. Chem.* **2019**, *7*, 671. (b) Tian, L.; et al. Carbon quantum dots for advanced electrocatalysis. *J. Energy Chem.* **2021**, *55*, 279−294. (c) Lim, S. Y.; Shen, W.; Gao, Z. Carbon quantum dots and their applications. *Chem. Soc. Rev.* **2015**, *44*, 362−381.

(20) Li, H.; et al. Carbon quantum dots with photo-generated proton property as efficient visible light controlled acid catalyst. *Nanoscale* **2014**, *6*, 867−873.

(21) Barman, S.; Sadhukhan, M. Facile bulk production of highly blue fluorescent graphitic carbon nitride quantum dots and their application as highly selective and sensitive sensors for the detection of mercuric and iodide ions in aqueous media. *J. Mater. Chem.* **2012**, *22*, 21832−21837.

(22) Zheng, M.; Liu, S.; Li, J.; Qu, D.; Zhao, H.; Guan, X.; Hu, X.; Xie, Z.; Jing, X.; Sun, Z. Integrating oxaliplatin with highly luminescent carbon dots: An unprecedented theranostic agent for personalized medicine. *Adv. Mater.* **2014**, *26*, 3554−3560.

(23) Li, H.; Liu, R.; Lian, S.; Liu, Y.; Huang, H.; Kang, Z. Near-infrared light controlled photocatalytic activity of carbon quantum dots for highly selective oxidation reaction. *Nanoscale* **2013**, *5*, 3289−3297.

(24) (a) Li, D.; Han, D.; Qu, S.-N.; Liu, L.; Jing, P.-T.; Zhou, D.; Ji, W.-Y.; Wang, X.-Y.; Zhang, T.-F.; Shen, D.-Z. Supra-(carbon nanodots) with a strong visible to near-infrared absorption band and efficient photothermal conversion. *Light: Sci. Appl.* **2016**, *5*, No. e16120. (b) Ge, J.; Jia, Q.; Liu, W.; Guo, L.; Liu, Q.; Lan, M.; Zhang, H.; Meng, X.; Wang, P. Red-emissive carbon dots for fluorescent, photoacoustic, and thermal theranostics in living mice. *Adv. Mater.* **2015**, *27*, 4169−4177.

(25) Wang, Y.; Meng, H.-M.; Song, G.; Li, Z.; Zhang, X.-B. Conjugated-polymer-based nanomaterials for photothermal therapy. *ACS Appl. Polym. Mater.* **2020**, *2*, 4258−4272.

(26) Jia, X.; Li, J.; Wang, E. One-pot green synthesis of optically pH-sensitive carbon dots with upconversion luminescence. *Nanoscale* **2012**, *4*, 5572−5575.

(27) Odian, G. Radical chain polymerization. In *Principles of Polymerization*; 3rd ed.; John Wiley & Sons, Ltd., 2004; pp. 198−349, DOI: 10.1002/047147875X.ch3.

(28) Beyler, C. L.; Hirschler, M. M. Thermal decomposition of polymers. In *SFPE Handbook of Fire Protection Engineering 2*; Springer, 2002; pp. 111−131.

(29) Arias-Rotondo, D. M.; McCusker, J. K. The photophysics of photoredox catalysis: A roadmap for catalyst design. *Chem. Soc. Rev.* **2016**, *45*, 5803−5820.

(30) (a) Huang, Z.; Shanmugam, M.; Liu, Z.; Brookfield, A.; Bennett, E. L.; Guan, R.; Herrera, D. E. V.; Lopez-Sanchez, J. A.;

Slater, A. G.; McInnes, E. J. L.; Qi, X.; Xiao, J. Chemical recycling of polystyrene to valuable chemicals via selective acid-catalyzed aerobic oxidation under visible light. *J. Am. Chem. Soc.* **2022**, *144*, 6532−6542. (b) Oh, S.; Stache, E. E. Chemical upcycling of commercial polystyrene via catalyst-controlled photooxidation. *J. Am. Chem. Soc.* **2022**, *144*, 5745−5749. (c) Zhang, G.; Zhang, Z.; Zeng, R. Photoinduced $FeCl_3$-catalyzed alkyl aromatics oxidation toward degradation of polystyrene at room temperature. *Chin. J. Chem.* **2021**, *39*, 3225−3230.

(31) Lutz, J. P.; Davydovich, O.; Hannigan, M. D.; Moore, J. S.; Zimmerman, P. M.; McNeil, A. J. Functionalized and degradable polyphthalaldehyde derivatives. *J. Am. Chem. Soc.* **2019**, *141*, 14544−14548.

(32) Scaiano, J. C.; Encinas, M. V.; George, M. V. Photochemistry of *o*-phthalaldehyde. *J. Chem. Soc. Perkin Trans. 2* **1980**, 724−730.

(33) (a) Kaminsky, W.; Franck, J. Monomer recovery by pyrolysis of poly(methyl methacrylate) (PMMA). *J. Anal. Appl. Pyrolysis* **1991**, *19*, 311−318. (b) Braido, R. S.; Borges, L. E. P.; Pinto, J. C. Chemical recycling of crosslinked poly(methyl methacrylate) and characterization of polymers produced with the recycled monomer. *J. Anal. Appl. Pyrolysis* **2018**, *132*, 47−55.

(34) Masutani, K.; Kimura, Y. PLA synthesis. From the monomer to the polymer. In *Poly(lactic acid) Science and Technology: Processing, Properties, Additives, and Applications*; Jimènez, A.; Peltzer, M. A.; Ruseckaite, R. A., Eds.; RSC Polymer Chemistry Series, No. 12; The Royal Society of Chemistry, 2014; pp. 1−36.

(35) Alberti, C.; Enthaler, S. Depolymerization of end-of-life poly(lactide) to lactide via zinc-catalysis. *ChemistrySelect* **2020**, *5*, 14759−14763.

(36) Savoldelli, J.; Tomback, D.; Savoldelli, H. Breaking down polystyrene through the application of a two-step thermal degradation and bacterial method to produce usable byproducts. *Waste Manage.* **2017**, *60*, 123−126.

(37) Lu, C.; Xiao, H.; Chen, X. Simple pyrolysis of polystyrene into valuable chemicals. *e-Polymers* **2021**, *21*, 428−432.

(38) (a) Zhang, Z.; Hirose, T.; Nishio, S.; Morioka, Y.; Azuma, N.; Ueno, A.; Ohkita, H.; Okada, M. Chemical recycling of waste polystyrene into styrene over solid acids and bases. *Ind. Eng. Chem. Res.* **1995**, *34*, 4514−4519. (b) Ukei, H.; Hirose, T.; Horikawa, S.; Takai, Y.; Taka, M.; Azuma, N.; Ueno, A. Catalytic degradation of polystyrene into styrene and a design of recyclable polystyrene with dispersed catalysts. *Catal. Today* **2000**, *62*, 67−75. (c) Adnan; Shah, J.; Jan, M. R. Thermo-catalytic pyrolysis of polystyrene in the presence of zinc bulk catalysts. *J. Taiwan Inst. Chem. Eng.* **2014**, *45*, 2494−2500.

https://doi.org/10.1021/jacs.3c04448
J. Am. Chem. Soc. 2023, 145, 16090−16097